Neuron
Article

Basal Ganglia Beta Oscillations Accompany Cue Utilization

Daniel K. Leventhal,[1] Gregory J. Gage,[2] Robert Schmidt,[2] Jeffrey R. Pettibone,[2] Alaina C. Case,[2] and Joshua D. Berke[2,*]
[1]Department of Neurology
[2]Department of Psychology
University of Michigan, Ann Arbor, MI 48109, USA
*Correspondence: jdberke@umich.edu
DOI 10.1016/j.neuron.2011.11.032

SUMMARY

Beta oscillations in cortical-basal ganglia (BG) circuits have been implicated in normal movement suppression and motor impairment in Parkinson's disease. To dissect the functional correlates of these rhythms we compared neural activity during four distinct variants of a cued choice task in rats. Brief beta (~20 Hz) oscillations occurred simultaneously throughout the cortical-BG network, both spontaneously and at precise moments of task performance. Beta phase was rapidly reset in response to salient cues, yet increases in beta power were not rigidly linked to cues, movements, or movement suppression. Rather, beta power was enhanced after cues were used to determine motor output. We suggest that beta oscillations reflect a postdecision stabilized state of cortical-BG networks, which normally reduces interference from alternative potential actions. The abnormally strong beta seen in Parkinson's Disease may reflect overstabilization of these networks, producing pathological persistence of the current motor state.

INTRODUCTION

Strong beta-band (~15–30 Hz) local field potential (LFP) oscillations are found in the BG and cortex of both humans with Parkinson's disease (PD; Weinberger et al., 2009; Levy et al., 2002; Hammond et al., 2007; Brown et al., 2001) and dopamine-lesioned animals (Mallet et al., 2008b; Sharott et al., 2005). Beta power is reduced by treatments that improve bradykinesia and rigidity, including dopamine replacement therapy (Levy et al., 2002; Brown et al., 2001) and deep brain stimulation (Kühn et al., 2008; Wingeier et al., 2006). Conversely, artificially driving the subthalamic nucleus or motor cortex at beta frequencies slows movement (Chen et al., 2007; Pogosyan et al., 2009). From these observations it has been hypothesized that beta oscillations in cortical-BG circuits are central to the systems-level pathophysiology of PD (Hammond et al., 2007; Weinberger et al., 2009), perhaps by interfering with the highly decorrelated patterns of neuronal spiking proposed to characterize normal BG information processing (Nini et al., 1995).

However, beta oscillations are also observed in multiple brain regions of awake, healthy subjects, including the sensorimotor neocortex of nonhuman primates (Murthy and Fetz, 1992; Sanes and Donoghue, 1993), mouse hippocampus (Berke et al., 2008), rat olfactory circuits (Kay et al., 2009), and the striatum in rats (Berke et al., 2004), nonhuman primates (Courtemanche et al., 2003), and humans (Sochurkova and Rektor, 2003). Cortical beta power is elevated during maintenance of a static position (Baker et al., 1997), active suppression of movement initiation (Swann et al., 2009), and postmovement hold periods (Pfurtscheller et al., 1996). Conversely, cortical beta power has been observed to decrease during movement preparation and initiation (Pfurtscheller et al., 2003; Zhang et al., 2008). These results have been taken as evidence that beta oscillations reflect "maintenance of the status quo" in the motor system (Engel and Fries, 2010). This concept fits well with the proposed pathophysiological role of beta oscillations in PD, where patients have difficulty not only initiating movement, but also in stopping or switching between motor programs (Stoffers et al., 2001). However, studies of beta oscillations within BG circuits have usually involved subjects that were anesthetized, dopamine-depleted, or not engaged in specific behaviors, so the natural correlates of BG beta oscillations are not well defined.

Here we investigate the functional correlates of BG beta oscillations in intact, unrestrained rats. We recorded simultaneously from multiple structures to assess whether beta rhythms coordinate activity throughout the BG network. The rats performed four task variants that make different demands for behavioral control: subjects were instructed to promptly make specific movements ("Immediate-GO"), program movements but delay their execution ("Deferred-GO"), inhibit movements ("NOGO"), or cancel movements-in-preparation ("STOP"). By comparing beta power time courses under each condition, we examined how dynamic states of cortical-BG circuits relate to distinct sensorimotor subprocesses.

RESULTS

Increased Beta Power Accompanies Action Programming

We first examined LFPs recorded from the striatum (STR), globus pallidus (GP), and primary motor cortex (M1) during a choice reaction time task. Rats initiated trials by poking and holding their position within an illuminated nose-port (Figures 1A and 1B). After a variable interval, one of two instruction

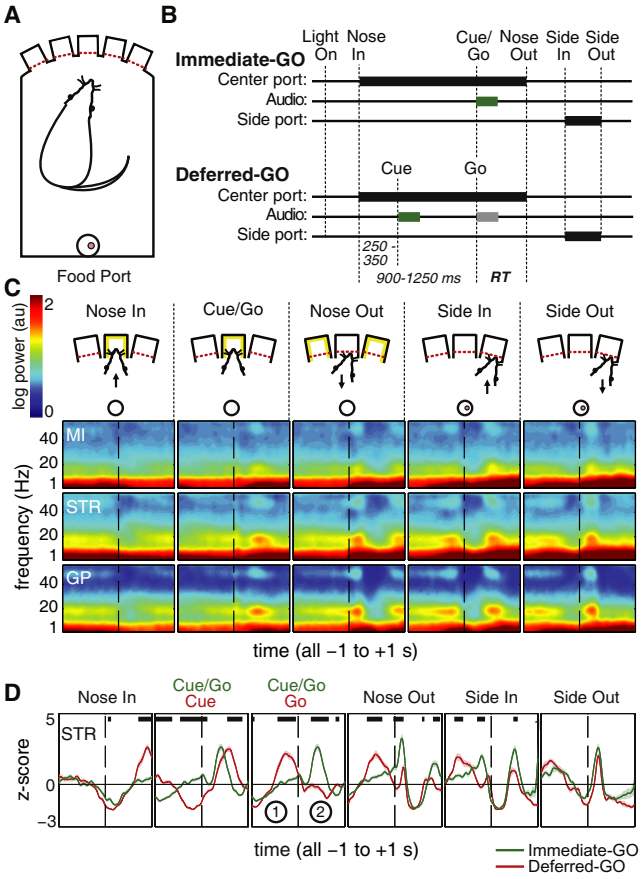

Figure 1. Cortical-BG Beta ERSs Are Induced by Instruction Cues, but Not by Movement Initiation or Immobility

(A) Schematic diagram of the five nose-port operant chamber with a food receptacle at the back. Broken red lines indicate photobeams.

(B) Event sequence for correct Immediate-GO and Deferred-GO trials. In both tasks, tone cues (green bars) instruct left or right movements. In the Immediate-GO task, these tones also serve as a Go cue, but in the Deferred-GO task subjects must wait until a separate signal to move (white noise; gray bar). Thick black bars indicate occupancy of a nose-port. RT, reaction time.

(C) LFP beta power (~20 Hz) is modulated with a similar time course in primary motor cortex (M1), striatum (STR), and globus pallidus (GP) during behavioral task performance. Event-triggered spectrograms were averaged across all Immediate-GO sessions (M1: 21 recording sites / 17 sessions / 3 rats, STR: 30 sites / 21 sessions / 5 rats, GP: 13 sites / 12 sessions / 3 rats). The color scale is logarithmic with respect to an arbitrary baseline.

(D) Mean beta (15–25 Hz) power z-scores in the striatum for all Immediate-GO and Deferred-GO sessions (Deferred-GO: 120 sites / 35 sessions / 4 rats). For the Immediate-GO task the "Cue/Go" panel is repeated for ease of comparison. Note that in both tasks rats are immobile during the epoch marked ①, and initiating movement during epoch ② (see also Figures S1C and S1D), yet at both times beta power is high for one task and low for the other. Shaded areas indicate the standard error of the mean. Black bars at the top of each panel indicate significant differences between beta power in the Immediate- and Deferred-GO tasks ($p < 0.001$, see Supplemental Experimental Procedures for details). See Figures S1A and S1B for recording sites.

cues (1 kHz, 4 kHz tones) directed the rat to quickly move his nose one port to the left or right, respectively. We have previously shown that contralateral performance in this "Immediate-GO" task is dependent on intact function of sensorimotor striatum (Gage et al., 2010).

Beta oscillations (15–25 Hz) were consistently more pronounced in STR and GP compared to M1, yet in each structure beta power was similarly modulated by task events (Figure 1C). Beta power initially dipped as rats entered the first port and stayed there (Nose In). This was followed by a sharp beta increase ("event-related synchronization," ERS) after the instruction tone (Cue/Go), which peaked just after they initiated their chosen movement (Nose Out). There was a further abrupt decrease in beta power (an "event-related desynchronization," ERD) as rats completed this movement (Side In), which triggered an audible food pellet delivery click on correct trials.

Movement initiation is typically associated with beta ERDs, in contrast to the ERS that we observed. However, most prior studies have either used self-paced movements (Pfurtscheller et al., 2003; Alegre et al., 2005) or imposed a delay between instruction cues and the corresponding movements (MacKay and Mendonça, 1995; Baker et al., 1997; Rubino et al., 2006; Sanes and Donoghue, 1993; Kühn et al., 2004). We therefore examined beta power during a second task version ("Deferred-GO," Figure 1B). In this task, subjects can use the instruction cue to prepare a movement, but to obtain reward they must delay execution until presentation of a separate "Go" signal. Information about the behavior of each rat in each task is given in Table S1 (available online). Rats trained in the Immediate-GO and Deferred-GO tasks attempted similar numbers of trials per session (averaging 173 and 160, respectively), consistent with similar levels of motivation.

In the Deferred-GO task the patterns of beta power (Figure 1D) more closely matched prior studies of nonhuman primate sensorimotor cortex (Sanes and Donoghue, 1993; MacKay and Mendonça, 1995; Rubino et al., 2006; Baker et al., 1997) and human subthalamic nucleus (Williams et al., 2003). For both tasks we observed a beta ERS several hundred milliseconds after instruction cue onset, even though the behaviors occurring at this time were very different (moving for Immediate-GO, holding for Deferred-GO). Conversely, some key epochs with similar overt behavior between tasks were associated with very different levels of beta power. This is most obvious around the time of Go cues (third panel of Figure 1D), for which rats in both tasks were maintaining a hold in the initial nose-port during epoch "1," and initiating movement during epoch "2."

Providing advance information about movement direction affects reaction times (RTs) (Luce, 1986). We examined individual RT distributions (Figures S1C and S1D) to assess their contribution to beta power differences between tasks. Rats performing the Deferred-GO task had bimodal RT distributions consistent with their sometimes reacting to the Go cue, but sometimes anticipating it (Gage et al., 2010). Strikingly, there was a beta ERS after the Go cue only for long-RT (>300 ms; presumed reactive) trials. On short-RT (<300 ms; presumed anticipatory) trials we found a beta ERD instead. During the Immediate-GO task, for which the rats do not know which way to go until the Cue/Go event, the beta ERS was observed for both long- and short-RT trials.

From the Immediate- and Deferred-GO tasks, we draw several interim conclusions. First, beta power increases are not simply

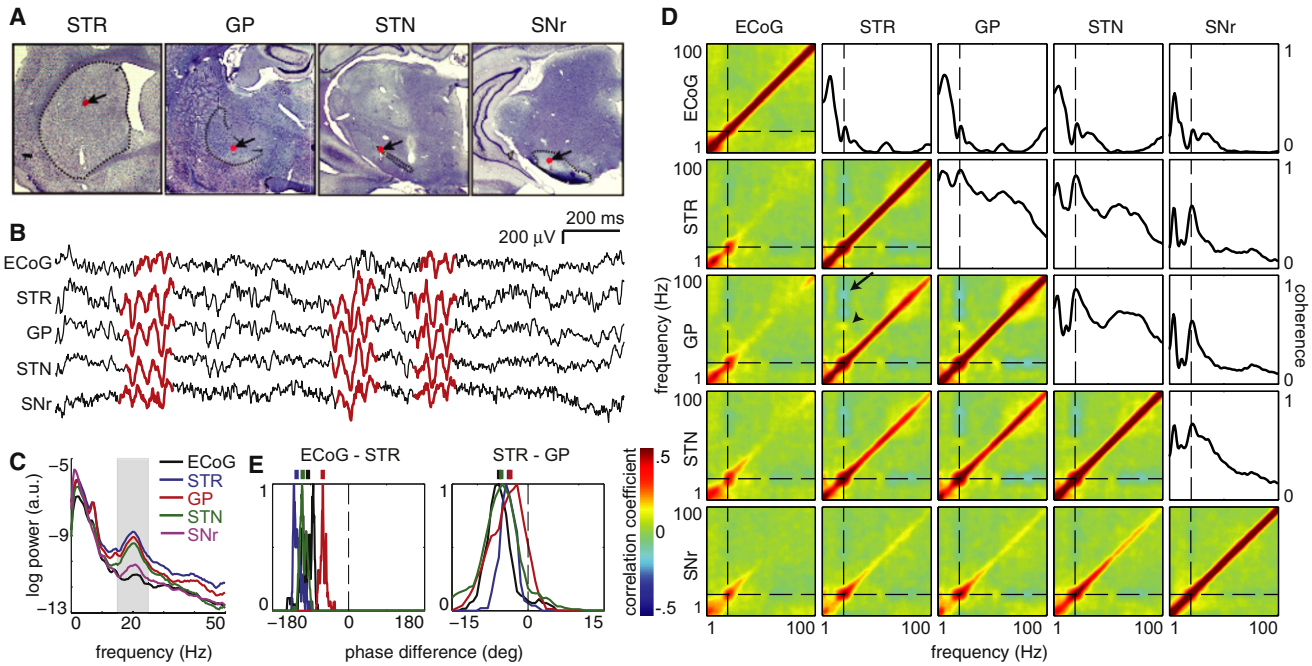

Figure 2. Selective Coordination of Beta Oscillations throughout Cortical-BG Networks

(A) Example of simultaneous recording sites in STR, GP, subthalamic nucleus (STN), and substantia nigra pars reticulata (SNr).

(B) LFP traces from the sites in (A), together with frontal ECoG. Red color highlights periods of elevated beta power, detected independently at each site (see Experimental Procedures).

(C) Mean power spectra from each recording site in (A) during a single session of Go/NoGo task performance. Gray shading indicates 15–25 Hz.

(D) Corresponding pairwise power comodulograms (colored panels) and coherence spectra (line plots). Dashed lines indicate 20 Hz. The arrow indicates negative correlation between beta and high gamma (~80 Hz), while the arrowhead indicates positive correlation between beta and low gamma (~50 Hz) power (note that this is not apparent between STR ~20 Hz and SNr ~50 Hz).

(E) Histograms of phase differences between frontal ECoG and STR (left), and STR and GP (right) during all simultaneous beta episodes. Each colored histogram represents a different rat, and is normalized to the peak count for that animal. Tick marks above each plot indicate median phase differences. See also Figure S3.

associated with holding position during delay periods, since in neither task did we see increased beta as subjects waited for the instruction cue. Second, beta power increases are not simply associated with movement, since the instruction cue produced a very similar beta ERS regardless of whether the instructed movement was performed immediately or was deferred. Third, presentation of a salient, task-relevant cue is not sufficient, since the beta ERS only followed the Go cue when the rats reacted to this cue, rather than having already anticipated it. Also inconsistent with a purely sensory response is the tighter locking of the beta ERS to movement onset than to the cue on Immediate-GO trials (Figure 1D).

Beta Oscillations Are Selectively Coordinated throughout the Basal Ganglia

To further investigate the functional correlates of BG beta oscillations, another group of rats was tested during two additional task variants ("Go/NoGo," "Stop-Signal"). These closely resembled the Immediate-Go task but incorporated cued movement suppression on some trials. To assess the organization of beta oscillations within the BG, implants targeted STR, GP, subthalamic nucleus (STN), and substantia nigra pars reticulata (SNr; Figures 2A and Figures S3A), together with a frontal electrocorticogram (ECoG). We found that beta oscillations occur simultaneously throughout the BG network (Figure 2B), in ~100–200 ms epochs (Figure S2A) that involve the cortical site as well. In plots of power spectral density (Figure 2C), each rat had peak BG beta frequency slightly below 20 Hz (range: 17.9–19.5 Hz) with cortical frequency consistently a touch higher (18.4 Hz to 20.4 Hz).

If beta oscillations represent a distinct, network-wide coordinated BG state, this should be apparent in analyses of phase and power relationships between structures. Coherence between all BG structures consistently showed a peak at ~20 Hz for all rats (Figures 2D and Figures S3B). By contrast, we have previously shown that coherence between striatum and dorsal hippocampus in behaving rats is close to zero at 20 Hz (Berke et al., 2004; Berke, 2009). We next constructed comodulograms, which illustrate the extent to which moment-to-moment oscillatory power covaries between structures (Buzsáki et al., 2003). Coordinated power changes within the BG network were observed especially at ~20 Hz (Figures 2D and Figures S3B). Modulation of beta power relative to behavioral events was essentially identical throughout the BG, and similar between BG and ECoG (Figure S2B). There was no consistent difference in the modulation of beta power for ipsilateral versus contralateral movements (Figure S4).

We have previously reported that striatal LFPs show mutually exclusive dynamic states, characterized by combinations of

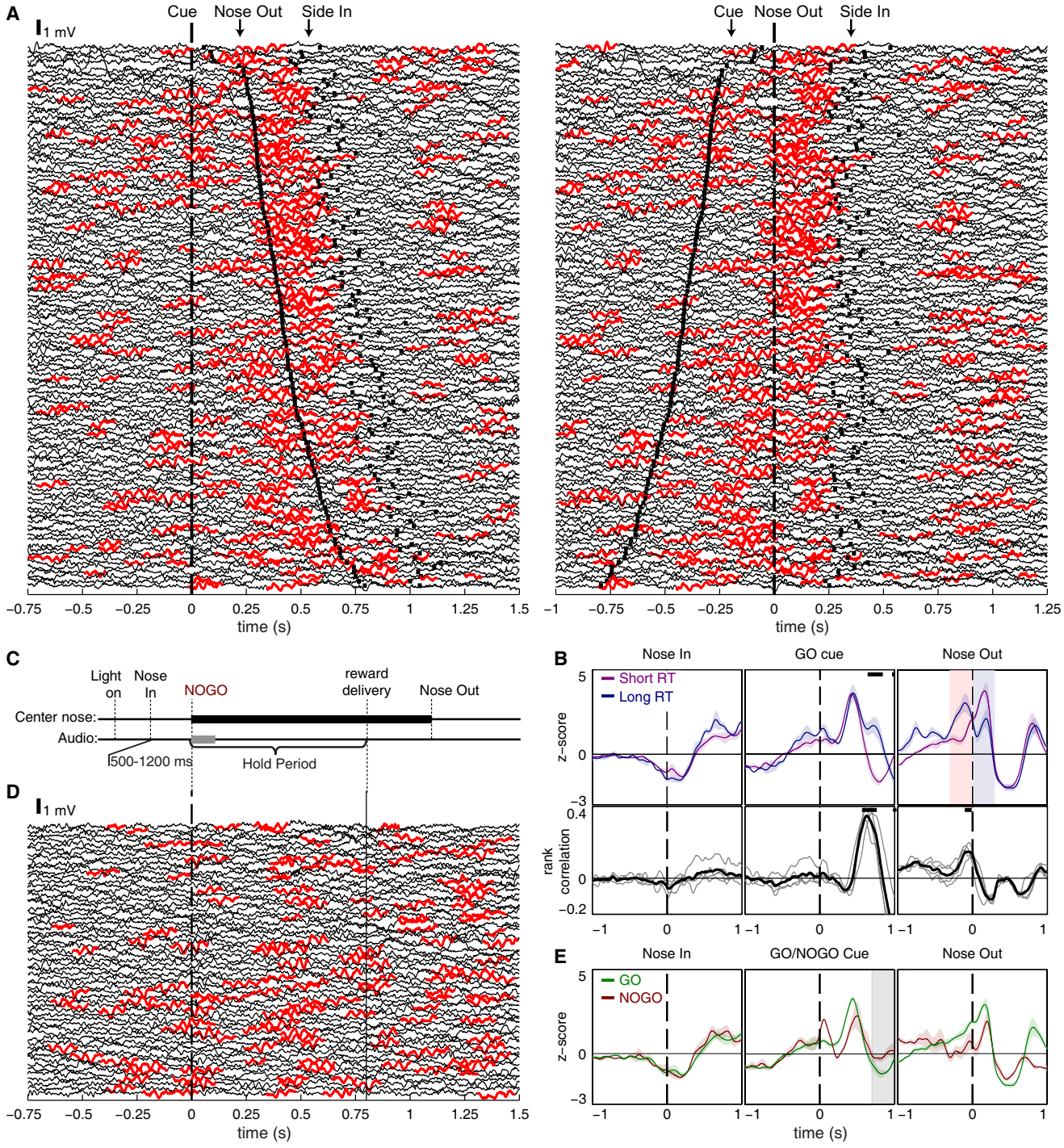

Figure 3. Beta Power Is Correlated with Reaction Time and Increases after Both Go and NoGo Cues

(A) Individual LFP traces from a STR site during GO trials in a single session, sorted by reaction time (RT). Left: GO trials aligned on instruction cue (dashed vertical line); the first and second black tick marks indicate the Nose Out and Side In events, respectively. Right: GO trials aligned on the Nose Out event; the first and second black tick marks indicate the instruction cue and Side In events, respectively. Note that beta oscillations are almost always present after the Nose Out event, but tend to occur before the Nose Out event only on trials with long RTs.

(B) Top: STR beta comparing short (<500 ms) and long (>500 ms) reaction time GO trials (including both Go/NoGo and Stop-signal sessions; 381 sites / 108 sessions / 4 rats). During the highlighted 300 ms epochs preceding and following Nose Out, all individual rats had significantly different beta power for short- and long-RT trials. Bottom: Spearman's rank correlations between local beta power and RT at each time point during task performance. Black bars indicate epochs of significant power differences (top) or correlations (bottom) for each individual rat at $p < 0.001$.

either ~20 Hz beta and ~50 Hz low-gamma rhythms, or ~8 Hz theta and ~80 Hz high-gamma rhythms, respectively (Berke, 2009; see also Dejean et al., 2011). These distinct states were visible in our current comodulograms: in STR, GP, and STN ~50 Hz power was positively correlated with beta power and negatively correlated with ~80 Hz activity. These relationships were absent or diminished for SNr.

BG beta rhythms were tightly coordinated between structures, but not identical in all respects. We consistently observed a significant difference in beta phase between simultaneously recorded subregions (28 pairwise comparisons, $p < 0.05$ in every case; see Experimental Procedures). Although the specific set of recording regions varied between subjects, for all four rats we were able to compare beta phases between frontal ECoG, STR, and GP (Figure 2E). STR beta was always phase-advanced relative to the ECoG, (by an average of 97°), and GP was always slightly phase-advanced relative to the striatum (by an average of 4.8°). These results rule out some nonphysiological explanations for coordinated beta rhythms throughout the BG—for example, if the beta oscillations were on the common reference electrode, they would show no phase shift across regions. However, phase differences do not necessarily indicate where an ERS/ERD occurs first, especially as beta has a different phase at the cortical surface compared to deep layers (Murthy and Fetz, 1992). We therefore also examined the slopes of the phase spectra between the ECoG, STR, and GP at beta frequencies (Figure S3C), which provides a measure of signal delay (Brown et al., 1998). The consistently very shallow slopes indicate that beta oscillations emerge with only small time delays throughout the cortical-BG network. Overall, our results are consistent with ~20 Hz beta having a selective, distinct role in coordinating information processing within the BG of normal behaving animals.

The Timing of Beta States Is Linked to Reaction Time

To explore beta timing in more detail, we examined trial-by-trial LFP traces during GO trials (Figure 3A). Epochs of high beta power appeared to occur stochastically, with some task events either increasing (Cue) or diminishing (Side In) the probability of entering this beta state. Around detected movement onset (Nose Out) the pattern of beta power change was unexpectedly complex, showing a marked dependence on reaction time. For the most rapid responses, the beta ERS began around the time of movement onset and peaked shortly afterwards (Figures 3A and 3B). On trials with slower responses, the beta ERS began well *before* movements and was mostly completed by movement onset. To quantify this phenomenon we compared beta power for fast- versus slow-RT trials during the 300 ms epochs immediately preceding and following movement onset (Figure 3B, top). In both epochs all subjects had a significant difference in beta power (paired t tests before Nose out: for 3 rats $p < 10^{-4}$, for the other $p = 0.024$; after Nose out: $p < 10^{-3}$ for all rats). In addition, we calculated correlation coefficients between beta power and reaction time at each moment during task performance (Figure 3B, bottom). A strong positive correlation was found about 750 ms after the Cue event, driven by the ERD that is maximal around movement completion (see Kühn et al., 2004; Williams et al., 2005 for related observations in humans). In addition, a smaller but reliable correlation occurred ~30–100 ms before movement initiation. This suggests that the presence of the high-beta state during a critical period delays movement onset, consistent with evidence in humans associating increased beta power with slower movements (Levy et al., 2002; Brown et al., 2001; Chen et al., 2007; Pogosyan et al., 2009).

Planning Not to Move Is Also Associated with Beta Increases

The Go/NoGo task variant (Figure 3C) is similar to the Immediate-Go task, except that there are three possible instruction cues: Go left, Go right, or hold in place (NoGo). As before, simply holding before the instruction cue was not associated with elevated beta. However, both Go and NoGo cues were similarly followed after several hundred milliseconds by a beta ERS (Figures 3D and 3E). This observation suggests that planning *not* to move is also associated with enhanced beta and confirms that the main beta ERS that we analyze here is not rigidly linked to either movement initiation or suppression. At the same time, we observed two interesting differences between GO and NOGO trials. First, the beta ERS to the NoGo cue was not followed by the marked ERD seen on GO trials, consistent with a more direct relationship between beta ERD and movement. Second, we noticed that the NoGo cue provoked an additional beta ERS with very low latency, and this was of consistently higher power in the frontal ECoG compared to BG sites (Figure S2C).

Enhanced Beta Power Occurs If Cues Are Used

The Stop-signal task is widely used to assess cognitive/executive function (Barch et al., 2009). Rats were cued to quickly Go left or Go right, but on a subset of trials (30%) a subsequent Stop signal told them to cancel and remain in the initial nose-port. The interval between the first Go cue and the Stop signal (stop-signal delay) was adjusted between sessions to find a point at which rats were sometimes able to countermand their action-in-preparation (STOP-Success trials) and sometimes not (STOP-Failure trials; Figure 4A). Comparing these trial types allows us to examine how identical sets of external cues can lead to different behavioral outcomes.

Performance in our version of the Stop-signal task (Table S1) was comparable to prior studies in humans (Swann et al., 2011), monkeys (Stuphorn et al., 2000), and rats (Feola et al., 2000; Eagle and Robbins, 2003). Consistent with theoretical "race" models (Logan et al., 1984), reaction times on STOP-Failure trials (Figure 4B) were similar to the early part of the GO trial reaction time distribution (trials with no Stop signal). As in

(C) Event sequence for correct NOGO trials (GO trials use the same sequence as Immediate-GO trials, Figure 1B). In this task, white noise (gray bar) is used as the NoGo cue. "Reward delivery" indicates the time at which the food hopper is audibly activated.
(D) NOGO trials from a STR site in a single recording session sorted by trial order. The solid vertical line indicates Reward Delivery (end of the required hold period).
(E) Mean z-scores (±SEM, shading) of STR beta power during correct GO (green) and NOGO (brown) trial performance (191 sites / 54 sessions / 4 rats). The gray band represents the range of limited hold durations across all recording sessions. See also Figure S2.

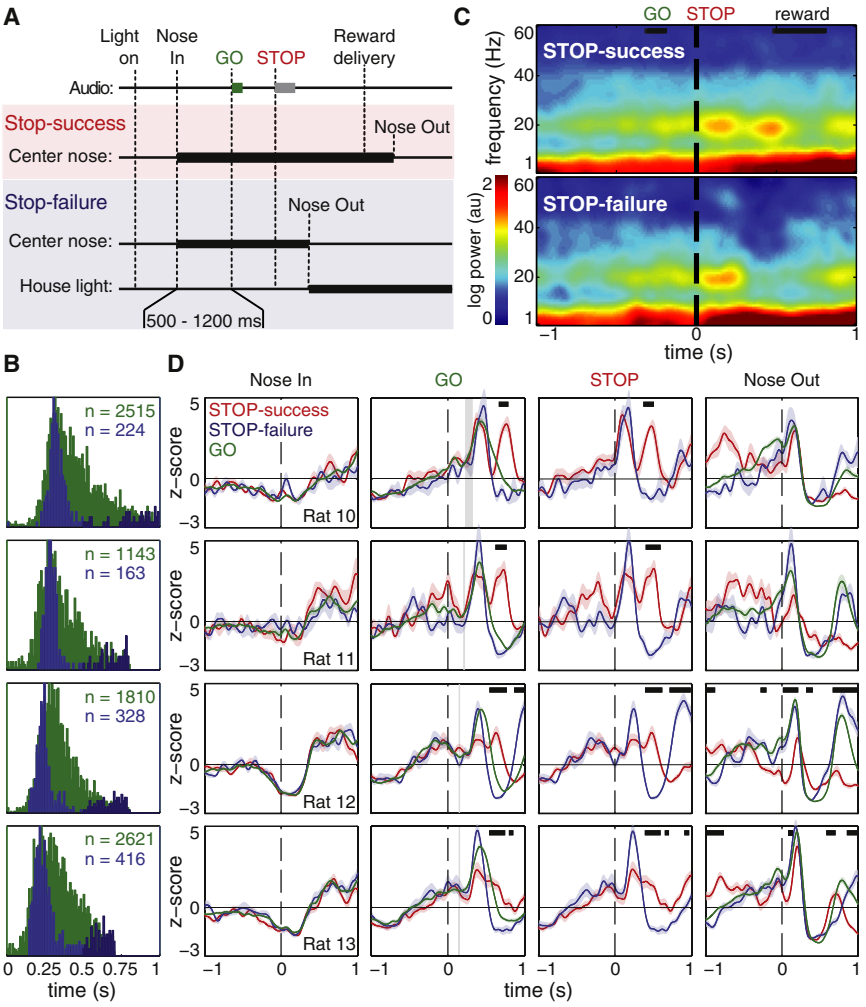

Figure 4. Beta Oscillations Only Follow Instruction Cues If the Cues Are Used

(A) Event sequence for successful and unsuccessful action cancellation (STOP trials, 30% of total; GO trials are the same as in the previous task variants). Green and gray bars indicate Go cue (tone) and Stop-signal (white noise).

(B) Normalized reaction time distributions for each rat on correct GO (green) and failed STOP (blue) trials during all stop-signal sessions. The distinctly distributed very slow STOP-failure trials (>500 ms; dark blue) are likely those in which the rat successfully arrested its movement but then moved prematurely to collect reward, and were excluded from subsequent analyses. Inset numbers indicate the total number of trials of each type.

(C) Mean Gabor spectrograms from one GP tetrode in a single rat (12 sessions), comparing successful (top) and failed (bottom) stopping. The vertical dashed line indicates the onset of the STOP-signal (white noise). Black bars at the top indicate time ranges for Go cue and reward delivery. The color scale is logarithmic with respect to an arbitrary baseline.

(D) Mean GP beta power z-scores during Stop-signal task performance, comparing STOP-success (red), STOP-failure (blue), and GO (green) trials. Gray bars indicate the range of stop-signal delays for each animal. Black lines at the top of each plot indicate significant differences between STOP-success and STOP-failure z-scores ($p < 0.001$; see Supplemental Experimental Procedures). See also Table S1.

each of our other task variants, presentation of the first instruction cue was always followed by a pronounced beta ERS. However, we found a striking difference between STOP-Success and STOP-Failure trials: only successful stopping was associated with a *second* abrupt increase in beta power (Figure 4c,d). This second beta pulse appeared to be the same cue-induced phenomenon as the first pulse that followed Go cues, as it had the same ~20 Hz frequency and followed the Stop-signal with a similar latency. Critically, however, the appearance of the second pulse only on STOP-Success trials confirms that mere presentation of a salient auditory cue is not sufficient to induce beta. Rather, the cue has to be actually used by the animal to affect behavioral output. This is consistent with observations of greater beta power in human frontal cortex for successful compared to failed stopping (Swann et al., 2009). However, in our experiments the beta ERS was seen following all cues that successfully directed behavioral output, including Go cues and even the food-hopper click at reward delivery (at "Side In" in Figures 1C and 1D). This transient increase in beta therefore appears to be related not specifically to action cancellation, but to a more general process induced whenever cues are used.

Distinct Processes of Beta Phase Reset and Power Change

Sensory cues can reset the phase of ongoing cortical oscillations (Makeig et al., 2004; Lakatos et al., 2007), including beta in motor cortex (Reimer and Hatsopoulos, 2010). We investigated whether the beta ERS is associated with, or separate to, such a phase reset. We found a strong, transient beta phase reset immediately following each auditory stimulus (Figures 5 and S5) that was present throughout the BG as well as the frontal ECoG. This phase reset was highly specific to the beta band at the cortical site and was seen for both beta and theta/alpha (~10 Hz) frequencies in the BG (Figures 5B and 5F). However, the reset had markedly lower latency than the main beta ERS and seemed instead to co-occur with the smaller, earlier beta ERS that was most prominent in the ECoG. Unlike the later changes in beta power, we saw equivalent beta phase resets to the Stop cue on *both* STOP-success and STOP-failure trials (no difference in orientation or magnitude of the mean resultant vector at any recording site, $p > 0.05$ with correction for multiple comparisons). Since this beta phase reset occurred regardless of whether the Stop cue determined behavior, we conclude that it is a distinct phenomenon that reflects an earlier, more "sensory" stage of sensorimotor processing than the strong beta ERS that accompanies cue utilization.

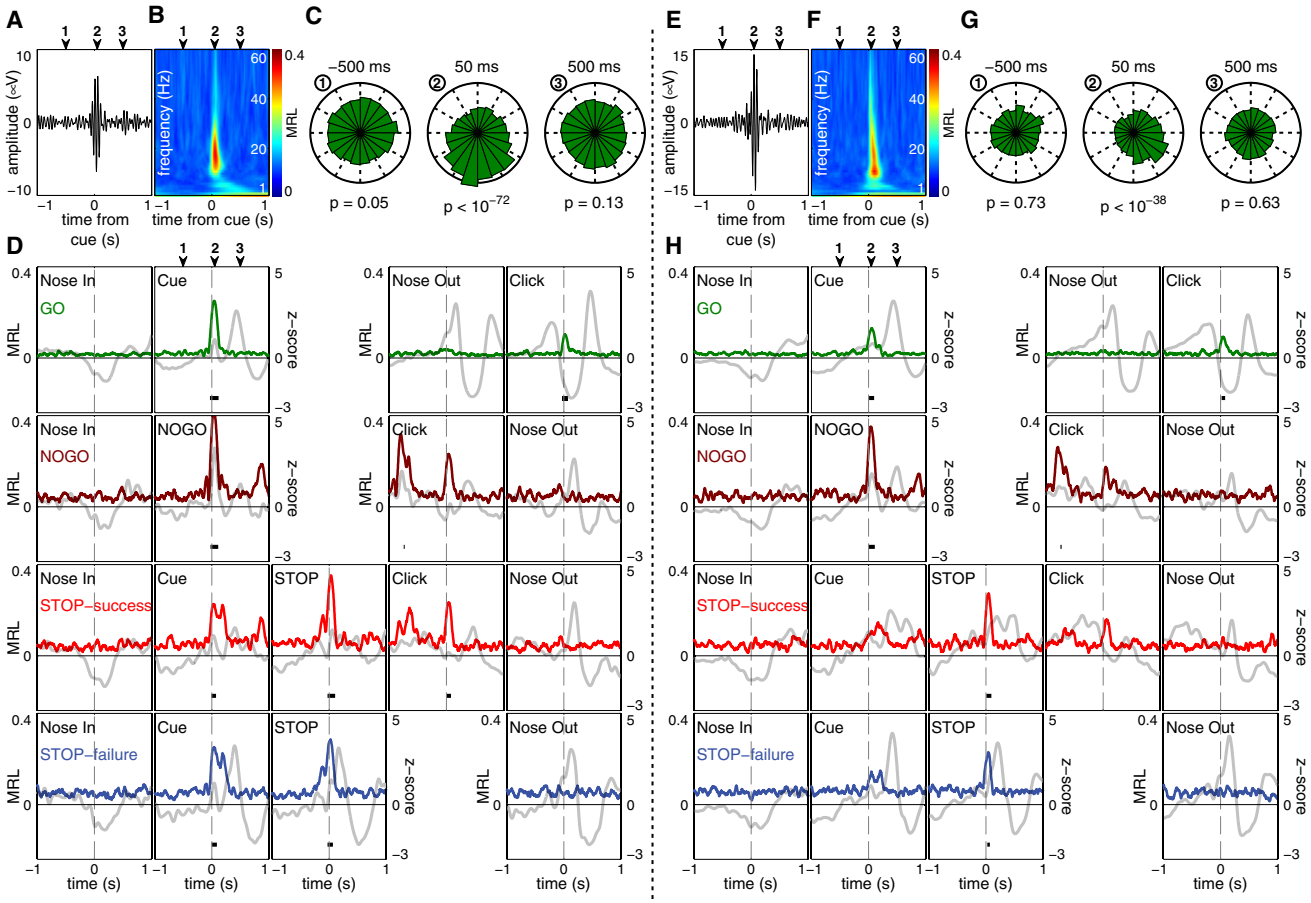

Figure 5. Relationship of Beta Phase to Task Events

(A) Average of the beta (15–25 Hz) filtered ECoG around the instruction cue during correctly performed GO trials, for a single animal across all sessions. The increased amplitude immediately after the cue indicates transiently consistent beta phase.

(B) Corresponding time-frequency plot of mean resultant length (MRL), indicating that the phase reset is selective to beta frequencies.

(C) Histograms of beta phases at selected time points. Note that beta phase is uniformly distributed at ±500 ms, but not at +50 ms. p values are for the Rayleigh test. The outer circles represent 350 counts. Calculations are for 5203 trials across 37 sessions.

(D) Time course of beta MRL (left axes) averaged across all rats. Overlaid gray lines are beta power z-scores (right axes) for the same task conditions. Note that every cue stimulus (instruction cue, STOP-signal, and food hopper click) is associated with phase reorganization, but this may or may not be associated with a subsequent increase in beta power. Black bars under each plot indicate epochs in which the MRL for each rat is significantly different from zero (Rayleigh test, $p < 0.001$).

(E–H) The same plots for striatal LFPs. See also Figure S5.

Neurons throughout the Basal Ganglia Participate in the Beta State

We and others have previously shown that individual BG neurons can become entrained to beta oscillations (Berke, 2005, 2009; Mallet et al., 2008b; Howe et al., 2011), but also that obvious strong entrainment is relatively rare in intact, behaving animals. To assess the potential impact of beta oscillations on information processing we examined spike-LFP phase relationships in each BG structure during beta epochs. We first tested whether each individual cell has a single preferred phase of firing relative to local beta (see Experimental Procedures). In each subregion (STR, GP, STN, SNr) we observed examples of neurons with highly significant phase preferences (Figure 6A). Across the four tasks, 82/830 units (9.9%) reached significance (Rayleigh test, $\alpha = 0.05$; Figure 6B). Next, we considered whether this set of cells tended to fire together during beta by examining the distribution of their preferred phases relative to the striatal beta rhythm. We found a clear preference at the population level for firing shortly before the positive peak of the striatal beta oscillation (Figure 6C; mean phase for entrained cells = 331°). This population-level preference was similar for each structure considered separately (STR projection cells, mean phase Φ = 349°, p = 0.0051; GP, Φ = 270°, p = 0.0099; STN, Φ = 274°, p = 0.013; SNr, Φ = 307°, p = 0.083).

These observations clearly demonstrate that beta rhythms are relevant to the firing patterns of BG neurons. At the same time, they confirm prior findings that beta is not dominating the activity of most neurons, most of the time. However, our data also provide two reasons to think that the above analyses understate the impact of beta on single-unit activity. First, when we

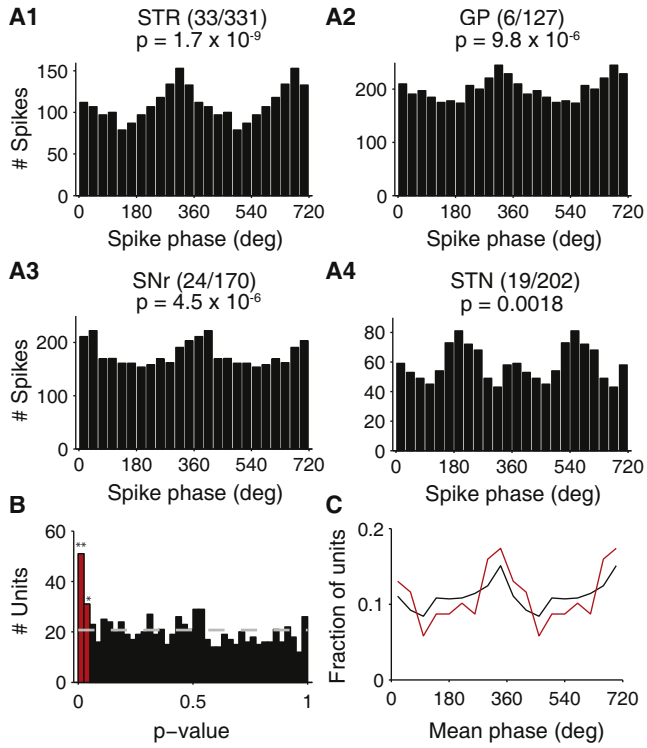

Figure 6. Beta-Entrainment of BG Neurons

(A1–A4) Phase histograms for four individual single units, showing spike timing relative to detected local beta oscillations (positive peaks at 0/360/720°), and associated significance p values. Note that the Rayleigh test used is sensitive only to single-peaked distributions, while the STN unit appears to have two preferred phases. Numbers in parentheses indicate proportions of entrained units in each area.

(B) A greater proportion of BG units are beta-entrained than expected by chance (*p = 0.02, **p = 8 × 10^{-9}; binomial test). Bins with p values below 0.05 are marked red, indicating the individually-entrained subpopulation. Gray dashed line indicates chance level.

(C) Distribution of individual cell phase preferences (relative to striatal beta peaks). The red line is for the population of cells that were individually entrained to striatal beta, while the black line is for the rest of the population. The overall population of BG units has a significant preferred mean phase just before the peak of striatal beta oscillations (p = 4 × 10^{-4}, Rayleigh test). See also Figure S6.

examined the preferred phase for the population of cells that did not individually reach significance, we found that it is identical to the significantly entrained cells (Figure 6C). This strongly suggests that a substantially larger group of cells also participates in the same beta rhythms, but we lacked statistical power to detect this when considering cells individually. Second, we observed clear cases of neurons that were not significantly entrained during all beta epochs, yet became powerfully entrained around specific task events (Figure S6). Beta may therefore contribute to BG information processing through the transient and selective formation of neuronal ensembles that are only weakly apparent in session-wide analyses. Further examination of such nonstationary entrainment may require new analyses that allow rhythmicity to be assessed in brief epochs involving small numbers of spikes (e.g., Dodla and Wilson, 2010).

DISCUSSION

We have presented two main findings about the dynamic organization of cortical-BG circuits. First, we have demonstrated that clear, discrete bursts of beta oscillations occur simultaneously throughout the BG of normal behaving rats and modulate the firing patterns of individual neurons. Second, we have shown that this state of elevated beta power reflects not simply sensory processing, or motor output, but rather occurs as subjects use sensory cues to determine voluntary actions. These results have important implications for our understanding of both normal BG function and PD.

Beta Oscillations and Parkinson's Disease

High beta power and coherence have been repeatedly observed in the cortex and BG following chronic dopamine depletion, leading to the idea that such oscillations are a key circuit-level driver of bradykinesia and rigidity in PD. Our results do not directly test this theory, but indicate that a state of elevated beta power and coordination between cortex and BG circuits occurs naturally at specific brief moments of behavioral task performance (see also Klostermann et al., 2007). Based on current evidence, it seems reasonable to consider the altered dynamics observed in PD not as inherently pathological, but rather as a network becoming stuck in one of a set of normal dynamic states. The highly regulated, transient nature of BG beta oscillations in intact animals may have contributed to their relative lack of prominence during spontaneous behavior (Mallet et al., 2008b; Sharott et al., 2005), compared to more active task engagement.

In rats, dopamine depletion leads to increased BG LFP power at, or slightly below, 20 Hz (Mallet et al., 2008b)—an excellent frequency match to the present results. In PD, dopaminergic therapy suppresses beta oscillations and in some patients causes the appearance of high-gamma oscillations instead (Brown et al., 2001). Similarly, we have previously shown that ~20 Hz (and ~50 Hz) oscillations in intact rat striatum are suppressed by dopaminergic drugs, which cause a prolonged shift toward the high-gamma state (Berke, 2009). A similar but more transient shift is also seen following natural rewards (Berke, 2009). Overall, our findings are consistent with increases and decreases in dopamine levels respectively pushing the BG away from, or toward, a dynamic state characterized by beta oscillations.

Despite the likely connection to dopamine signaling, rapid decreases in dopamine levels are not sufficient for the appearance of BG beta oscillations. Beta is not typically observed following acute administration of dopamine antagonists (Mallet et al., 2008b; Burkhardt et al., 2007) and takes days to weeks to develop following dopamine-depleting 6-OHDA lesions (Mallet et al., 2008b; Degos et al., 2009). This progressive change may involve structural remodeling of striatal microcircuits, including altered connectivity between fast-spiking interneurons and projection cells (Gittis et al., 2011). Ongoing experience is also likely to play a role both in the progressive increase in beta and the development of specific behavioral deficits. For example, following unilateral 6-OHDA lesions in a similar operant task performance is initially normal, but continued task

experience produces a progressive decline in contralateral action selection (Dowd and Dunnett, 2007).

Origins and Timing of Basal Ganglia Beta

Our LFP analysis has significant limitations. Determining the cellular-synaptic mechanisms underlying LFP oscillations is especially challenging in structures that lack clear cell layers (Berke, 2005). In both PD patients and dopamine-depleted rats, array-type probes have been used to demonstrate that the power of beta oscillations is greater in STN than just above or below (Mallet et al., 2008b; Weinberger et al., 2006; Kühn et al., 2005) and a similar approach would be useful in intact task-performing rats.

The beta ERS to an instruction cue was highly consistent despite variability in exact recording sites between different animals and task variants. Although we recorded simultaneously from multiple neural targets, microelectrode neurophysiology does not allow complete brain coverage. We therefore cannot entirely rule out the possibility that beta is even stronger and more functionally relevant in locations that we did not examine, and spreads passively into the BG (Sirota et al., 2008). However, our observations that oscillatory coordination within the BG (and between cortex and BG) is quite selective for beta rhythms, and that a significant number of BG cells are strongly modulated by beta rhythms, provide solid evidence that beta is important for the functional organization of these circuits.

Several features of BG anatomy and physiology potentially contribute to coordinated changes in beta oscillations. Neurons of the intralaminar thalamus have early access to salient sensory stimuli (Matsumoto et al., 2001) and some have branching axons that innervate STR, GP, and STN (Deschênes et al., 1996; Castle et al., 2005). In humans STN also receives inputs from cortical regions important for response inhibition (Aron et al., 2007) that show beta band oscillations following stop-signal cues (Swann et al., 2009). STN in turn provides rapid excitatory input to multiple BG sites, targeting neurons even outside the usual constraints imposed by topographic organization (Parent and Hazrati, 1995). Finally, the GP (GPe in primates) provides broadly targeted GABAergic input to the whole BG (Kita, 2007). GP input has been shown in brain slices to reset the phase of autonomous spiking within the STN (Baufreton et al., 2005), and resonant feedback between GP and STN has been repeatedly proposed as an oscillatory mechanism (Bevan et al., 2002; Holgado et al., 2010; Mallet et al., 2008a). Determining how BG interconnections contribute to behavior-linked beta change is an important challenge for future studies.

We observed multiple, dissociable relationships between beta processes and behavioral events. First, each of the auditory cues resulted in very rapid beta phase reset, often without simultaneous changes in beta power. Reset of ongoing rhythms by salient cues has been previously reported in multiple cortical regions, for a range of oscillatory frequencies including beta (Lakatos et al., 2007). Such resets are largely independent of sensory modality, and have been proposed to reflect a rapid modulatory process that causes incoming sensory information to arrive in cortex when neurons are at a phase of peak excitability. The resulting facilitation of sensory processing may help reduce reaction times to attended instruction cues (Senkowski et al., 2006). Similarly, within monkey primary motor cortex the appearance of a visual reach target, and/or an associated auditory cue, provokes very rapid beta reset (Reimer and Hatsopoulos, 2010) that appears to be the same reset phenomenon that we observed throughout cortical-BG circuits. Such a coordinated phase reset may enhance effective communication between regions (Fries, 2005). Both the short latency of the phase reset (within tens of milliseconds) and the fact that the reset to Stop cues did not differentiate between Stop-success and Stop-failure trials indicate that this aspect of cortical-BG coordination is linked to early stages of sensory processing.

Each of the auditory cues used in the task was also followed by an increase in beta power, with a latency of several hundred milliseconds. However, this beta ERS appeared only if the cues influenced behavioral output. Such selectivity was seen in two distinct situations: first, the beta ERS to the Stop cue occurred on Stop-success but not Stop-failure trials, and second, in the Deferred-Go task the beta ERS to the Go cue occurred only when the rats used this external cue to prompt their responses, rather than performing self-timed movements. These complementary observations clearly demonstrate that the beta ERS is not simply related to sensory processing. Nor is it simply related to movement, or the absence of movement. Beta power was reduced below baseline as animals held still while waiting for an instruction cue. Once this cue occurred, we saw an equivalent beta ERS whether rats initiated action (in the Immediate-GO condition) or continued to hold (in the Deferred-GO and NOGO conditions). Therefore, there is no consistent relationship between the presence or absence of BG beta oscillations and the motor state of the subject, and merely maintaining an existing motor state is not sufficient to generate enhanced beta power. Our results are instead consistent with a role for beta oscillations in "sensorimotor integration" (Baker, 2007; Lalo et al., 2007). Similar results have been reported in the STN of parkinsonian humans (Williams et al., 2003), where an instruction cue resulted in a beta ERS only if it was informative about the direction of a subsequent required movement.

By contrast, the strong ERD seen after the ERS on Immediate-GO trials appeared more directly linked to motor performance. The ERD was present as rats performed the left/right movement in all trial types, with a straightforward relationship to reaction times, and was absent following cues that successfully prompted animals not to move. A movement-linked beta ERD is consistent with many previous studies of human sensorimotor cortex (Jasper and Penfield, 1949), although in our experiments it occurred slightly later than expected—near completion of the brief movement rather than initiation.

The relatively long latency of the beta ERS places further constraints on its potential functional significance. As it typically occurred at, or just after, the fastest reaction times, the beta ERS does not appear to be a necessary link in a serial chain of subprocesses using sensory input to select and initiate motor output (Meyer et al., 1988). Similarly, it is unlikely that the beta ERS is causally involved in cue-evoked cancellation of movements, as in our Stop-signal task the second beta peak occurred substantially after the "stop-signal reaction time" (SSRT, Table S1 and Figure 4D), an inferred measure of the speed of action cancellation (Logan et al., 1984). Despite this relatively slow

pace of cue-evoked beta power change, there was a clear relationship between the presence of beta oscillations and ongoing behavior, with higher beta power preceding more slowly initiated movements (see also Chen et al., 2007; Pogosyan et al., 2009).

Beta Rhythms and the Status Quo

Our present data are consistent with observations that cortical-BG circuits show both spontaneous and regulated transitions between discrete dynamic states (Berke, 2009), at least one of which is characterized by high beta power. We suggest that beta represents a relatively "stabilized" state during which a change in behavioral program is less likely. As brain circuits establish behavioral plans, entry into the stabilized state would serve the adaptive function of reducing interference from other salient cues and competing alternative actions. Conversely, premature or unregulated entry into beta at critical moments would tend to retard the preparation of intended actions, contributing to both natural reaction time variation in normal subjects, and movement difficulties in PD.

This view of beta oscillations builds upon extensive prior findings and theoretical discussion. Observations of beta ERDs with movement (also seen here), together with elevated beta in PD, led to the idea that beta rhythms in cortical-BG circuits are "antikinetic." In its simplest form, this implies that beta should be low as movements are initiated, and high as they are suppressed. Yet we found no single relationship between overt movement and beta power: movement onset was often coincident with elevated beta, and maintaining a fixed position was often coincident with lowered beta. Similarly, the simplest reading of the hypothesis that sensorimotor beta is important for "maintaining the status quo" is incompatible with our data, if the relevant metric is taken to be movement. NoGo and Go cues provoked a similar beta ERS, despite the fact that the NoGo cue instructed subjects to maintain the current motor program and the Go cue prompted a new movement.

More sophisticated accounts of sensorimotor beta have focused on movement change, rather than movement per se. For example, Gilbertson et al. (2005) suggested that beta synchrony "might herald a cortical state, albeit temporary, in which any processing of new movements is impaired," and similarly Engel and Fries (2010) wrote, "beta-band activity may be a signature of an active process that promotes the existing motor set whilst compromising neuronal processing of new movements." Our proposal here is closely related, yet places this prior idea in a more general, functional context. We suggest that entry into the high-beta state naturally accompanies cue utilization, as cortical-BG circuits stabilize representations of selected behavioral programs. This stabilization would compromise not only the processing of new movements, but also other behavioral programs such as movement suppression. This may be the reason why while training each rat in the Stop-signal task, the stop-signal delay consistently converged on a point just before the beta ERS induced by the Go cue (Figures 4C and 4D). If the Stop cue was given later (i.e., during the ERS) the proportion of successful Stop trials was very low. In future studies we intend to more directly examine the role of beta in the stabilization of neural representations, for example by looking at trial-to-trial variability in the firing patterns of both single neurons (Berke, 2011) and large ensembles of cells during movement preparation (Afshar et al., 2011).

Our working hypothesis is that this stabilized cortico-BG beta state is related to gating functions of the BG, in both sensorimotor processing (Hikosaka and Wurtz, 1985) and other operations like working memory (Frank et al., 2001). Gating is a critical function for adaptive, flexible behavior, not least because it allows a separation between the salience of stimuli and their motivational impact on behavior (Brown et al., 2004). For example, it can be important not to react to cues as quickly as possible when there may be conflicting additional cues coming, or as the meaning of those cues changes. We propose that high beta power reflects a relatively "closed" BG gate. A major acute function of dopamine may be to encourage gate opening (Ivry and Spencer, 2004) so that cues appropriately energize/motivate behavior (Hikosaka, 2007; Mazzoni et al., 2007). In PD, dopaminergic medication suppresses beta power and facilitates movement, but also causes problems including impulsivity and difficulty ignoring distracting cues (Cools et al., 2003; Moustafa et al., 2008). Similarly, in rats, enhancement of dopamine signaling with amphetamine or apomorphine causes suppression of beta power (Berke, 2009) and abnormalities in sensorimotor gating, as assessed by prepulse inhibition of acoustic startle (Ralph-Williams et al., 2002). As one possible test of our gating hypothesis, we predict an inverse relationship between beta power evoked by a prepulse and the startle response to the subsequent cue.

EXPERIMENTAL PROCEDURES

Behavioral Tasks

All animal procedures were approved by the University of Michigan Committee on Use and Care of Animals. Each group of rats was identically food-restricted during training and behavioral testing, receiving 15 g of standard laboratory rat chow daily (in addition to rewards received during task performance).

Immediate-GO Task

To start each trial one of the three central nose-ports was lit randomly, indicating that the rat should poke and hold its nose in that port (Figure 1B). After a variable delay, a cue tone (~65 dB) instructed the rat to move promptly into the immediately adjacent nose-port to the left (1 kHz tone) or right (4 kHz tone). Failure to hold until cue tone onset led to houselight illumination and a 10–15 s timeout. Successful trials were rewarded with a 45 mg fruit punch flavored sucrose pellet at the back of the chamber.

Deferred-GO Task

This task was identical to the immediate-GO task, except that after the instructional cue tone, the rats had to continue holding in the initial nose-port until a second "GO" cue (Gaussian white noise, 125 ms duration, intensity ~65 dB) played. The intervals between "Nose In" and the instructional cue, as well as between the instructional and GO cues, were variable.

Go/NoGo and Stop-Signal Tasks

Individual rats were tested on these tasks in separate sessions on alternating days. In both tasks, 70% of trials were "GO" trials, which were identical to the Immediate-GO task with minor exceptions (in particular, the instruction cue lasted just 50 ms). Other trials were either "NOGO" or "STOP" trials depending on the session. To encourage rats to respond as quickly as possible, on GO trials rats had to initiate the movement within a "limited hold" period (Table S1). Rats were also required to poke the adjacent port within a period tuned to the performance of each rat (termed the "movement hold") after leaving the initial nose-port. Incorrect performance caused houselight illumination for an 8 s timeout.

On NOGO trials, a white noise burst (125 ms duration) played instead of the pure tone; on STOP trials, the white noise burst played at a fixed interval

(the stop-signal delay, SSD) after the pure tone ("GO" cue). To successfully complete a NOGO or STOP trial, the rat had to maintain its nose in the initial port until the "limited hold" period would have expired on a GO trial. The SSD was tuned for each rat so that it would erroneously continue its movement (STOP-Failure) or successfully stop on approximately equal numbers of trials. During each test session, SSD was held constant to facilitate analysis of the electrophysiological data triggered on the GO and STOP cues.

Electrophysiology

Rats received implants containing 21 individually drivable tetrodes (Gage et al., 2010). For the Immediate- and Deferred-GO tasks, tetrodes were targeted to right M1, STR, and GP. For rats trained on the Go/NoGo and Stop-signal tasks, the left BG (STR, GP, STN, and SNr) were targeted. Ipsilateral prefrontal ECoGs were recorded with skull screws in contact with the brain (AP 4.5 mm, ML 1.5 mm relative to bregma). All signals were referenced to a skull screw on the midline 1 mm posterior to lambda (between cerebral cortex and cerebellum). We have found previously that this reference location is not itself associated with substantial beta power, that would produce artificially elevated beta coherence estimates between all pairs of forebrain locations (Berke, 2009).

Electrophysiological Data Analysis

Analyses were performed using Matlab (Mathworks, Inc., Natick, MA).

Time-Frequency Analysis

Gabor power spectrograms were computed by convolving LFPs with Gaussian-tapered (50 ms standard deviation) complex sinusoids of integer frequencies from 1 to 100 Hz, and taking the logarithm of the squared magnitude of the resulting time-series. To generate Figures 1C and Figures 4C, the spectrograms for each recording session were averaged. To generate power comodulograms (Figures 2D and Figures S3B), Pearson's correlation coefficient was calculated between these same time series for each pair of recording sites. This resulted in a 100 × 100 grid with each point having a value ranging from −1 (perfect anticorrelation of power at two frequencies) to +1 (perfect correlation of power at two frequencies). Only epochs during which the rat was engaged in the task (from initial nose poke to trial completion) were included.

Power and Coherence Spectra

Power spectra (Figure 2C) were calculated for each trial, averaged across trials to give a mean spectrum at each recording site for each session, and smoothed with a three-point rectangular sliding window. To calculate coherence spectra, for each trial we calculated the cross-spectrum between each pair of recording sites. Session-wide coherence was then calculated as the squared magnitude of the averaged trial-by-trial cross spectra normalized by the product of the average autospectra (Figure 2E).

Continuous Beta Power and Phase

See Figures 1D, Figures 3B, 3E; Figures 4D; Figures S2, S5. LFPs were zero-phase filtered between 15–25 Hz and the analytic signal was calculated using the Hilbert transform. The squared magnitude of the analytic signal is a continuous measure of beta power, and continuous beta phase was extracted as the argument of the analytic signal. To obtain z-scores for beta power on each tetrode in each recording session, a bootstrapping method was used (Canolty et al., 2007, see Supplemental Experimental Procedures).

For each pairwise combination of recording sites, overlapping epochs of identified beta oscillations were extracted to calculate interregional phase differences (see *Identification of beta epochs* in Supplemental Experimental Procedures). Beta phase was unwrapped to generate a time series of continuously increasing phase values. The mean phase difference for each overlap epoch was calculated, and these values were averaged to generate a mean phase difference between sites. The distribution of these session-wide phase differences (Figure 2E) was used to evaluate the overall beta phase difference between regions. Significance testing of the median phase of these distributions against the null hypothesis of zero-phase difference was performed using standard circular statistics (Berens, 2009).

The circular spread of beta phases at each time point was quantified by calculating the length of their mean resultant vector (the "mean resultant length," MRL) (Berens, 2009; Lakatos et al., 2007). MRLs were considered significantly different from zero for p values < 0.001 (Rayleigh test) that persisted for at least 50 ms consecutively. The distributions of beta phases on STOP-Success and -Failure trials were compared 50 ms after the STOP signal (see Supplemental Experimental Procedures). To generate the time-frequency MRL plots (Figures 5A and 5C), phase was extracted at integer frequencies from 1 to 100 Hz by convolving the LFP signal with Gaussian-tapered complex sinusoids and taking the argument of the resulting complex time series. The standard deviations of the Gaussian windows were related to the sinusoid frequency as $\sigma = 0.849 / f$, generating standard Morlet wavelets.

Phase Spectra

Cross-spectra for every pairwise combination of recording sites were calculated during overlapping periods of identified beta oscillations. The phase spectrum between each pair of sites was calculated as the argument of the mean cross-spectra across overlapping beta epochs. Mean phase spectra were calculated by taking the circular means of the phase spectra for each contact pair for a given region pair (i.e., all pairwise combinations of striatal and pallidal sites for Figure S3C, bottom) within each session, and these session-wide phase spectra were averaged to give mean phase spectra between regions for each rat (Figure S3C).

Correlation of Beta Power with RT

To generate Figure 3B (bottom), trials were pooled across recording session for each striatal tetrode. Beta power at each time point for each trial was correlated with RT using Spearman's rank correlation (ρ), due to the skewed nature of the RT distribution. Within each subject, ρ was averaged to yield the plots in Figure 3B. p values were determined using a large-sample approximation that ρ is normally distributed and were considered significant if p was less than 0.001 for all striatal sites for at least 50 ms consecutively. Nearly identical results were obtained using Pearson's correlation coefficient.

Spike-LFP Phase Histograms

Spike-phase histograms were constructed for single units with respect to the LFP recorded on the same tetrode during identified beta, and tested for nonuniformity with the Rayleigh test. Only units that yielded more than 50 spikes during beta epochs were included. Artificial spike:LFP phase locking can sometimes be produced when the same signal is used to extract action potentials and LFPs (Berke, 2005). To eliminate this possibility, we repeated the analysis after removing the action potentials from the filtered LFP signal by excising the time periods from 2 ms before to 4 ms after each spike, and substituting a linear interpolation (Jacobs et al., 2007). This procedure had no significant impact on the results, which are therefore reported for the unmodified LFPs.

SUPPLEMENTAL INFORMATION

Supplemental Information includes six figures, one table, and Supplemental Experimental Procedures and can be found with this article online at doi:10.1016/j.neuron.2011.11.032.

ACKNOWLEDGMENTS

The authors would like to thank members of the Berke laboratory for assistance with experiments and Roger Albin, Nicolas Mallet, and Daniel Weissman for their useful comments. This work was supported by the National Institute on Drug Abuse, the Whitehall Foundation, and the University of Michigan. D.K.L. was supported by National Institutes on Neurological Disorders and Stroke training grant NS007222 and National Institutes on Aging grant AG024824. R.S. was supported by DFG-grant SCHM 2745/1-1.

Accepted: November 27, 2011
Published: February 8, 2012

REFERENCES

Afshar, A., Santhanam, G., Yu, B.M., Ryu, S.I., Sahani, M., and Shenoy, K.V. (2011). Single-trial neural correlates of arm movement preparation. Neuron *71*, 555–564.

Alegre, M., Alonso-Frech, F., Rodríguez-Oroz, M.C., Guridi, J., Zamarbide, I., Valencia, M., Manrique, M., Obeso, J.A., and Artieda, J. (2005). Movement-related changes in oscillatory activity in the human subthalamic nucleus: ipsilateral vs. contralateral movements. Eur. J. Neurosci. *22*, 2315–2324.

Aron, A.R., Behrens, T.E., Smith, S., Frank, M.J., and Poldrack, R.A. (2007). Triangulating a cognitive control network using diffusion-weighted magnetic resonance imaging (MRI) and functional MRI. J. Neurosci. *27*, 3743–3752.

Baker, S.N. (2007). Oscillatory interactions between sensorimotor cortex and the periphery. Curr. Opin. Neurobiol. *17*, 649–655.

Baker, S.N., Olivier, E., and Lemon, R.N. (1997). Coherent oscillations in monkey motor cortex and hand muscle EMG show task-dependent modulation. J. Physiol. *501*, 225–241.

Barch, D.M., Braver, T.S., Carter, C.S., Poldrack, R.A., and Robbins, T.W. (2009). CNTRICS final task selection: executive control. Schizophr. Bull. *35*, 115–135.

Baufreton, J., Atherton, J.F., Surmeier, D.J., and Bevan, M.D. (2005). Enhancement of excitatory synaptic integration by GABAergic inhibition in the subthalamic nucleus. J. Neurosci. *25*, 8505–8517.

Berens, P. (2009). CircStat: a MATLAB toolbox for circular statistics. J. Stat. Softw. 31.

Berke, J.D. (2005). Participation of striatal neurons in large-scale oscillatory networks. In Basal Ganglia VIII, J.P. Bolam, C.A. Ingham, and P.J. Magill, eds. (New York, NY: Springer Science).

Berke, J.D. (2009). Fast oscillations in cortical-striatal networks switch frequency following rewarding events and stimulant drugs. Eur. J. Neurosci. *30*, 848–859.

Berke, J.D. (2011). Functional properties of striatal fast-spiking interneurons. Front Syst Neurosci *5*, 45.

Berke, J.D., Okatan, M., Skurski, J., and Eichenbaum, H.B. (2004). Oscillatory entrainment of striatal neurons in freely moving rats. Neuron *43*, 883–896.

Berke, J.D., Hetrick, V., Breck, J., and Greene, R.W. (2008). Transient 23-30 Hz oscillations in mouse hippocampus during exploration of novel environments. Hippocampus *18*, 519–529.

Bevan, M.D., Magill, P.J., Terman, D., Bolam, J.P., and Wilson, C.J. (2002). Move to the rhythm: oscillations in the subthalamic nucleus-external globus pallidus network. Trends Neurosci. *25*, 525–531.

Brown, P., Salenius, S., Rothwell, J.C., and Hari, R. (1998). Cortical correlate of the Piper rhythm in humans. J. Neurophysiol. *80*, 2911–2917.

Brown, P., Oliviero, A., Mazzone, P., Insola, A., Tonali, P., and Di Lazzaro, V. (2001). Dopamine dependency of oscillations between subthalamic nucleus and pallidum in Parkinson's disease. J. Neurosci. *21*, 1033–1038.

Brown, J.W., Bullock, D., and Grossberg, S. (2004). How laminar frontal cortex and basal ganglia circuits interact to control planned and reactive saccades. Neural Netw. *17*, 471–510.

Burkhardt, J.M., Constantinidis, C., Anstrom, K.K., Roberts, D.C., and Woodward, D.J. (2007). Synchronous oscillations and phase reorganization in the basal ganglia during akinesia induced by high-dose haloperidol. Eur. J. Neurosci. *26*, 1912–1924.

Buzsáki, G., Buhl, D.L., Harris, K.D., Csicsvari, J., Czéh, B., and Morozov, A. (2003). Hippocampal network patterns of activity in the mouse. Neuroscience *116*, 201–211.

Canolty, R.T., Soltani, M., Dalal, S.S., Edwards, E., Dronkers, N.F., Nagarajan, S.S., Kirsch, H.E., Barbaro, N.M., and Knight, R.T. (2007). Spatiotemporal dynamics of word processing in the human brain. Front Neurosci *1*, 185–196.

Castle, M., Aymerich, M.S., Sanchez-Escobar, C., Gonzalo, N., Obeso, J.A., and Lanciego, J.L. (2005). Thalamic innervation of the direct and indirect basal ganglia pathways in the rat: Ipsi- and contralateral projections. J. Comp. Neurol. *483*, 143–153.

Chen, C.C., Litvak, V., Gilbertson, T., Kühn, A., Lu, C.S., Lee, S.T., Tsai, C.H., Tisch, S., Limousin, P., Hariz, M., and Brown, P. (2007). Excessive synchronization of basal ganglia neurons at 20 Hz slows movement in Parkinson's disease. Exp. Neurol. *205*, 214–221.

Cools, R., Barker, R.A., Sahakian, B.J., and Robbins, T.W. (2003). L-Dopa medication remediates cognitive inflexibility, but increases impulsivity in patients with Parkinson's disease. Neuropsychologia *41*, 1431–1441.

Courtemanche, R., Fujii, N., and Graybiel, A.M. (2003). Synchronous, focally modulated beta-band oscillations characterize local field potential activity in the striatum of awake behaving monkeys. J. Neurosci. *23*, 11741–11752.

Degos, B., Deniau, J.M., Chavez, M., and Maurice, N. (2009). Chronic but not acute dopaminergic transmission interruption promotes a progressive increase in cortical beta frequency synchronization: relationships to vigilance state and akinesia. Cereb. Cortex *19*, 1616–1630.

Dejean, C., Arbuthnott, G., Wickens, J.R., Le Moine, C., Boraud, T., and Hyland, B.I. (2011). Power fluctuations in beta and gamma frequencies in rat globus pallidus: association with specific phases of slow oscillations and differential modulation by dopamine D1 and D2 receptors. J. Neurosci. *31*, 6098–6107.

Deschênes, M., Bourassa, J., Doan, V.D., and Parent, A. (1996). A single-cell study of the axonal projections arising from the posterior intralaminar thalamic nuclei in the rat. Eur. J. Neurosci. *8*, 329–343.

Dodla, R., and Wilson, C.J. (2010). A phase function to quantify serial dependence between discrete samples. Biophys. J. *98*, L5–L7.

Dowd, E., and Dunnett, S.B. (2007). Movement without dopamine: striatal dopamine is required to maintain but not to perform learned actions. Biochem. Soc. Trans. *35*, 428–432.

Eagle, D.M., and Robbins, T.W. (2003). Inhibitory control in rats performing a stop-signal reaction-time task: effects of lesions of the medial striatum and d-amphetamine. Behav. Neurosci. *117*, 1302–1317.

Engel, A.K., and Fries, P. (2010). Beta-band oscillations—signalling the status quo? Curr. Opin. Neurobiol. *20*, 156–165.

Feola, T.W., de Wit, H., and Richards, J.B. (2000). Effects of d-amphetamine and alcohol on a measure of behavioral inhibition in rats. Behav. Neurosci. *114*, 838–848.

Frank, M.J., Loughry, B., and O'Reilly, R.C. (2001). Interactions between frontal cortex and basal ganglia in working memory: a computational model. Cogn. Affect. Behav. Neurosci. *1*, 137–160.

Fries, P. (2005). A mechanism for cognitive dynamics: neuronal communication through neuronal coherence. Trends Cogn. Sci. (Regul. Ed.) *9*, 474–480.

Gage, G.J., Stoetzner, C.R., Wiltschko, A.B., and Berke, J.D. (2010). Selective activation of striatal fast-spiking interneurons during choice execution. Neuron *67*, 466–479.

Gilbertson, T., Lalo, E., Doyle, L., Di Lazzaro, V., Cioni, B., and Brown, P. (2005). Existing motor state is favored at the expense of new movement during 13-35 Hz oscillatory synchrony in the human corticospinal system. J. Neurosci. *25*, 7771–7779.

Gittis, A.H., Hang, G.B., LaDow, E.S., Shoenfeld, L.R., Atallah, B.V., Finkbeiner, S., and Kreitzer, A.C. (2011). Rapid target-specific remodeling of fast-spiking inhibitory circuits after loss of dopamine. Neuron *71*, 858–868.

Hammond, C., Bergman, H., and Brown, P. (2007). Pathological synchronization in Parkinson's disease: networks, models and treatments. Trends Neurosci. *30*, 357–364.

Hikosaka, O. (2007). Basal ganglia mechanisms of reward-oriented eye movement. Ann. N Y Acad. Sci. *1104*, 229–249.

Hikosaka, O., and Wurtz, R.H. (1985). Modification of saccadic eye movements by GABA-related substances. II. Effects of muscimol in monkey substantia nigra pars reticulata. J. Neurophysiol. *53*, 292–308.

Holgado, A.J., Terry, J.R., and Bogacz, R. (2010). Conditions for the generation of beta oscillations in the subthalamic nucleus-globus pallidus network. J. Neurosci. *30*, 12340–12352.

Howe, M.W., Atallah, H.E., McCool, A., Gibson, D.J., and Graybiel, A.M. (2011). Habit learning is associated with major shifts in frequencies of oscillatory activity and synchronized spike firing in striatum. Proc. Natl. Acad. Sci. USA *108*, 16801–16806.

Ivry, R.B., and Spencer, R.M. (2004). The neural representation of time. Curr. Opin. Neurobiol. *14*, 225–232.

Jacobs, J., Kahana, M.J., Ekstrom, A.D., and Fried, I. (2007). Brain oscillations control timing of single-neuron activity in humans. J. Neurosci. *27*, 3839–3844.

Jasper, H., and Penfield, W. (1949). Electrocorticograms in man: Effect of voluntary movement upon the electrical activity of the precentral gyrus. Eur. Arch. Psychiatry Clin. Neurosci. *183*, 163–174.

Kay, L.M., Beshel, J., Brea, J., Martin, C., Rojas-Líbano, D., and Kopell, N. (2009). Olfactory oscillations: the what, how and what for. Trends Neurosci. *32*, 207–214.

Kita, H. (2007). Globus pallidus external segment. Prog. Brain Res. *160*, 111–133.

Klostermann, F., Nikulin, V.V., Kühn, A.A., Marzinzik, F., Wahl, M., Pogosyan, A., Kupsch, A., Schneider, G.H., Brown, P., and Curio, G. (2007). Task-related differential dynamics of EEG alpha- and beta-band synchronization in cortico-basal motor structures. Eur. J. Neurosci. *25*, 1604–1615.

Kühn, A.A., Williams, D., Kupsch, A., Limousin, P., Hariz, M., Schneider, G.H., Yarrow, K., and Brown, P. (2004). Event-related beta desynchronization in human subthalamic nucleus correlates with motor performance. Brain *127*, 735–746.

Kühn, A.A., Trottenberg, T., Kivi, A., Kupsch, A., Schneider, G.H., and Brown, P. (2005). The relationship between local field potential and neuronal discharge in the subthalamic nucleus of patients with Parkinson's disease. Exp. Neurol. *194*, 212–220.

Kühn, A.A., Kempf, F., Brücke, C., Gaynor Doyle, L., Martinez-Torres, I., Pogosyan, A., Trottenberg, T., Kupsch, A., Schneider, G.H., Hariz, M.I., et al. (2008). High-frequency stimulation of the subthalamic nucleus suppresses oscillatory beta activity in patients with Parkinson's disease in parallel with improvement in motor performance. J. Neurosci. *28*, 6165–6173.

Lakatos, P., Chen, C.M., O'Connell, M.N., Mills, A., and Schroeder, C.E. (2007). Neuronal oscillations and multisensory interaction in primary auditory cortex. Neuron *53*, 279–292.

Lalo, E., Gilbertson, T., Doyle, L., Di Lazzaro, V., Cioni, B., and Brown, P. (2007). Phasic increases in cortical beta activity are associated with alterations in sensory processing in the human. Exp. Brain Res. *177*, 137–145.

Levy, R., Ashby, P., Hutchison, W.D., Lang, A.E., Lozano, A.M., and Dostrovsky, J.O. (2002). Dependence of subthalamic nucleus oscillations on movement and dopamine in Parkinson's disease. Brain *125*, 1196–1209.

Logan, G.D., Cowan, W.B., and Davis, K.A. (1984). On the ability to inhibit simple and choice reaction time responses: a model and a method. J. Exp. Psychol. Hum. Percept. Perform. *10*, 276–291.

Luce, R.D. (1986). Response Times: Their Role in Inferring Elementary Mental Organization (New York, NY: Oxford University Press).

MacKay, W.A., and Mendonça, A.J. (1995). Field potential oscillatory bursts in parietal cortex before and during reach. Brain Res. *704*, 167–174.

Makeig, S., Debener, S., Onton, J., and Delorme, A. (2004). Mining event-related brain dynamics. Trends Cogn. Sci. (Regul. Ed.) *8*, 204–210.

Mallet, N., Pogosyan, A., Márton, L.F., Bolam, J.P., Brown, P., and Magill, P.J. (2008a). Parkinsonian beta oscillations in the external globus pallidus and their relationship with subthalamic nucleus activity. J. Neurosci. *28*, 14245–14258.

Mallet, N., Pogosyan, A., Sharott, A., Csicsvari, J., Bolam, J.P., Brown, P., and Magill, P.J. (2008b). Disrupted dopamine transmission and the emergence of exaggerated beta oscillations in subthalamic nucleus and cerebral cortex. J. Neurosci. *28*, 4795–4806.

Matsumoto, N., Minamimoto, T., Graybiel, A.M., and Kimura, M. (2001). Neurons in the thalamic CM-Pf complex supply striatal neurons with information about behaviorally significant sensory events. J. Neurophysiol. *85*, 960–976.

Mazzoni, P., Hristova, A., and Krakauer, J.W. (2007). Why don't we move faster? Parkinson's disease, movement vigor, and implicit motivation. J. Neurosci. *27*, 7105–7116.

Meyer, D.E., Osman, A.M., Irwin, D.E., and Yantis, S. (1988). Modern mental chronometry. Biol. Psychol. *26*, 3–67.

Moustafa, A.A., Sherman, S.J., and Frank, M.J. (2008). A dopaminergic basis for working memory, learning and attentional shifting in Parkinsonism. Neuropsychologia *46*, 3144–3156.

Murthy, V.N., and Fetz, E.E. (1992). Coherent 25- to 35-Hz oscillations in the sensorimotor cortex of awake behaving monkeys. Proc. Natl. Acad. Sci. USA *89*, 5670–5674.

Nini, A., Feingold, A., Slovin, H., and Bergman, H. (1995). Neurons in the globus pallidus do not show correlated activity in the normal monkey, but phase-locked oscillations appear in the MPTP model of parkinsonism. J. Neurophysiol. *74*, 1800–1805.

Parent, A., and Hazrati, L.N. (1995). Functional anatomy of the basal ganglia. II. The place of subthalamic nucleus and external pallidum in basal ganglia circuitry. Brain Res. Brain Res. Rev. *20*, 128–154.

Pfurtscheller, G., Stancák, A., Jr., and Neuper, C. (1996). Post-movement beta synchronization. A correlate of an idling motor area? Electroencephalogr. Clin. Neurophysiol. *98*, 281–293.

Pfurtscheller, G., Graimann, B., Huggins, J.E., Levine, S.P., and Schuh, L.A. (2003). Spatiotemporal patterns of beta desynchronization and gamma synchronization in corticographic data during self-paced movement. Clin. Neurophysiol. *114*, 1226–1236.

Pogosyan, A., Gaynor, L.D., Eusebio, A., and Brown, P. (2009). Boosting cortical activity at Beta-band frequencies slows movement in humans. Curr. Biol. *19*, 1637–1641.

Ralph-Williams, R.J., Lehmann-Masten, V., Otero-Corchon, V., Low, M.J., and Geyer, M.A. (2002). Differential effects of direct and indirect dopamine agonists on prepulse inhibition: a study in D1 and D2 receptor knock-out mice. J. Neurosci. *22*, 9604–9611.

Reimer, J., and Hatsopoulos, N.G. (2010). Periodicity and evoked responses in motor cortex. J. Neurosci. *30*, 11506–11515.

Rubino, D., Robbins, K.A., and Hatsopoulos, N.G. (2006). Propagating waves mediate information transfer in the motor cortex. Nat. Neurosci. *9*, 1549–1557.

Sanes, J.N., and Donoghue, J.P. (1993). Oscillations in local field potentials of the primate motor cortex during voluntary movement. Proc. Natl. Acad. Sci. USA *90*, 4470–4474.

Senkowski, D., Molholm, S., Gomez-Ramirez, M., and Foxe, J.J. (2006). Oscillatory beta activity predicts response speed during a multisensory audio-visual reaction time task: a high-density electrical mapping study. Cereb. Cortex *16*, 1556–1565.

Sharott, A., Magill, P.J., Harnack, D., Kupsch, A., Meissner, W., and Brown, P. (2005). Dopamine depletion increases the power and coherence of beta-oscillations in the cerebral cortex and subthalamic nucleus of the awake rat. Eur. J. Neurosci. *21*, 1413–1422.

Sirota, A., Montgomery, S., Fujisawa, S., Isomura, Y., Zugaro, M., and Buzsáki, G. (2008). Entrainment of neocortical neurons and gamma oscillations by the hippocampal theta rhythm. Neuron *60*, 683–697.

Sochurkova, D., and Rektor, I. (2003). Event-related desynchronization/synchronization in the putamen. An SEEG case study. Exp. Brain Res. *149*, 401–404.

Stoffers, D., Berendse, H.W., Deijen, J.B., and Wolters, E.C. (2001). Motor perseveration is an early sign of Parkinson's disease. Neurology *57*, 2111–2113.

Stuphorn, V., Taylor, T.L., and Schall, J.D. (2000). Performance monitoring by the supplementary eye field. Nature *408*, 857–860.

Swann, N., Tandon, N., Canolty, R., Ellmore, T.M., McEvoy, L.K., Dreyer, S., DiSano, M., and Aron, A.R. (2009). Intracranial EEG reveals a time- and frequency-specific role for the right inferior frontal gyrus and primary motor cortex in stopping initiated responses. J. Neurosci. *29*, 12675–12685.

Swann, N., Poizner, H., Houser, M., Gould, S., Greenhouse, I., Cai, W., Strunk, J., George, J., and Aron, A.R. (2011). Deep brain stimulation of the subthalamic nucleus alters the cortical profile of response inhibition in the beta frequency band: a scalp EEG study in Parkinson's disease. J. Neurosci. *31*, 5721–5729.

Weinberger, M., Mahant, N., Hutchison, W.D., Lozano, A.M., Moro, E., Hodaie, M., Lang, A.E., and Dostrovsky, J.O. (2006). Beta oscillatory activity in the subthalamic nucleus and its relation to dopaminergic response in Parkinson's disease. J. Neurophysiol. *96*, 3248–3256.

Weinberger, M., Hutchison, W.D., and Dostrovsky, J.O. (2009). Pathological subthalamic nucleus oscillations in PD: can they be the cause of bradykinesia and akinesia? Exp. Neurol. *219*, 58–61.

Williams, D., Kühn, A., Kupsch, A., Tijssen, M., van Bruggen, G., Speelman, H., Hotton, G., Yarrow, K., and Brown, P. (2003). Behavioural cues are associated with modulations of synchronous oscillations in the human subthalamic nucleus. Brain *126*, 1975–1985.

Williams, D., Kühn, A., Kupsch, A., Tijssen, M., van Bruggen, G., Speelman, H., Hotton, G., Loukas, C., and Brown, P. (2005). The relationship between oscillatory activity and motor reaction time in the parkinsonian subthalamic nucleus. Eur. J. Neurosci. *21*, 249–258.

Wingeier, B., Tcheng, T., Koop, M.M., Hill, B.C., Heit, G., and Bronte-Stewart, H.M. (2006). Intra-operative STN DBS attenuates the prominent beta rhythm in the STN in Parkinson's disease. Exp. Neurol. *197*, 244–251.

Zhang, Y., Chen, Y., Bressler, S.L., and Ding, M. (2008). Response preparation and inhibition: the role of the cortical sensorimotor beta rhythm. Neuroscience *156*, 238–246.